

Optimal Fabrication Processes for Unidirectional Metal-Matrix Composites: A Computational Simulation

D.A. Saravanos
Case Western Reserve University
Cleveland, Ohio

P.L.N. Murthy
National Aeronautics and Space Administration
Lewis Research Center
Cleveland, Ohio

and

M. Morel
Sverdrup Technology, Inc.
NASA Lewis Research Center Group
Cleveland, Ohio

Prepared for the
35th International SAMPE Symposium and Exhibition
Anaheim, California, April 2-5, 1990



(NASA-TM-102559) OPTIMAL FABRICATION
PROCESSES FOR UNIDIRECTIONAL METAL-MATRIX
COMPOSITES: A COMPUTATIONAL SIMULATION
(NASA) 19 p

CSCL 110

N90-21143

Unclas

G3/24 0278785

OPTIMAL FABRICATION PROCESSES FOR UNIDIRECTIONAL METAL-MATRIX
COMPOSITES: A COMPUTATIONAL SIMULATION

D.A. Saravanos,*
Case Western Reserve University
Cleveland, Ohio 44106

P.L.N. Murthy
National Aeronautics and Space Administration
Lewis Research Center
Cleveland, Ohio 44135

and

M. Morel
Sverdrup Technology, Inc.
NASA Lewis Research Center Group
Cleveland, Ohio 44135

ABSTRACT

A method is proposed for optimizing the fabrication process of unidirectional metal-matrix composites. The temperature and pressure histories are optimized such that the residual microstresses of the composite at the end of the fabrication process are minimized and the material integrity throughout the process is ensured. The response of the composite during the fabrication is simulated based on a nonlinear micromechanics theory. The optimal fabrication problem is formulated and solved with non-linear programming. Application cases regarding the optimization of the fabrication cool-down phases of unidirectional ultra-high modulus graphite/copper and silicon carbide/titanium composites are presented.

NOMENCLATURE

E	Young's Modulus.
$F(\mathbf{z})$	Objective function.
G	Shear Modulus.
$Q(\mathbf{z})$	Inequality constraint.
$H(\mathbf{z})$	Equality constraint.
P	Property.

*NASA Resident Research Associate at Lewis Research Center.

p	Pressure.
S	Strength.
T	Temperature.
T_M	Melting temperature.
t	Time.
t_F	Time constant.
w_i	Weighting coefficients.
z	Optimization vector.
α	Thermal expansion coefficient.
ρ	Mass Density.
σ	Stress.
ν	Poisson's ratio.

Superscripts

A, B, C	Different regions in the unit cell.
L	Lower bound.
U	Upper bound.

Subscripts

C	Compression.
f	Fiber.
m	Matrix.
n	Normal.
o	Reference.
s	Shear.
T	Tension.
t	Final.
1, 2, 3	Composite material coordinate system axes.

1. INTRODUCTION

During the last few years, significant interest has developed for metal-matrix composite (MMC) materials. Despite their high cost, metal-matrix composites (MMCs) are promising candidate materials for applications demanding high operational temperatures (from 800°F to 2000°F), high specific stiffness and strength, hygrothermal resistance, stability, and tailorable mechanical properties. A problem with most MMCs is the high residual thermal microstresses developed during the cooling phase of the fabrication process. These high residual stresses are primarily caused by the large temperature differential imposed during the cooling phase because of the mismatch between the thermal expansion coefficients of the composite's constituents.

The development of thermal residual stresses during fabrication is a known problem for composite materials. Much research has been reported on the thermal residual microstresses of polymer-matrix composites. We selectively mention some early studies on thermal stresses of composite laminates [1-2], as well as, some studies on the prediction of residual stresses during the curing of thermoset-matrix composites [3] and during the solidification of thermoplastic-matrix composites [4-6]. However, the residual thermal stresses generally are more critical for MMCs than polymer matrix composites because of the much larger temperature differential involved in the fabrication of MMC's.

The residual microstresses degrade the mechanical properties of MMCs, may initiate matrix failures, and are primarily responsible for their poor thermo-mechanical fatigue endurance. Experimental and computational studies [7-8] indicate that in addition to other factors, the residual microstresses depend on the actual cool-down and consolidation histories during fabrication, since the metallic matrix undergoes in situ nonlinear deformations. The material behavior is further complicated by the fact that the in situ mechanical properties of the matrix depend on temperature and stress. Hence, a process may exist with optimal temperature and pressure variation, that will produce MMCs with favorable thermal residual stresses and improved thermo-mechanical fatigue (TMF) life.

To the authors' best knowledge, no research has been reported on the prediction of

optimal cooling and consolidation histories for MMCs. Research on the optimal fabrication process of polymer-matrix composites [9] has limited applicability because in most cases the highly non-linear matrix behavior is not an issue. The present paper describes recent studies on the development of a methodology for optimizing the fabrication parameters of unidirectional MMCs such that: (1) critical residual microstresses are minimized; and (2) failures in the matrix, fibers, and fiber/matrix interphase are prevented during fabrication. All these are directly related to TMF endurance and ensure its improvement, while item (2) also ensures the integrity of the composite.

The residual microstresses and the mechanical properties of the material are predicted based on integrated non-linear micromechanics for metal-matrix composites developed at the Lewis Research Center [10-11]. The optimization problem is formulated and solved with the modified feasible directions mathematical programming method. The material nonlinearity requires special considerations in the formulation and solution of the problem which are addressed herein. Applications of the developed methodology are performed on the optimization of the cool-down process of unidirectional silicon-carbide(SiC)/titanium (Ti15-3-3-3) and ultra high modulus graphite(P100)/copper composites.

2. FABRICATION PROCESS

The variety in properties of fibers and matrices, the size of the fibers, the chemical reactivity between fibers and matrix at higher temperatures, and the attained quality and properties of the final composite have resulted in the development of various fabrication techniques. Among them, superplastic diffusion bonding and hot isostatic pressing appear to have many merits and potential. A typical fabrication cycle, as the one shown in Fig. 1 for P100/copper, usually involves three phases. During Phase 1, the temperature of the raw materials is elevated near the matrix melting temperature. Application of consolidation pressure is usually required in Phase 2 such that the matrix is diffused and bonded with the fibers. It is assumed that Phase 2 is sufficiently long such that perfect bonding is accomplished and consolidation stresses are negligible. The final cool-down phase (Phase 3) follows in order to reduce the temperature and pressure to the reference conditions.

Phase 3 seems to be most critical in the subsequent performance of the fabricated MMC, in that the residual microstresses are substantially developed during this phase as a result of the mismatch between the fiber and matrix thermal expansion coefficients. Mechanical microstresses are also present as a result of the consolidation pressure. Part of the mechanical microstresses vanishes when the consolidation pressure is removed, however, their simultaneous action with the thermally induced microstresses may contribute to matrix failures. Since the development of residual stresses and the integrity of the composite material is primarily affected by the temperature and pressure histories in Phase 3, it is reasonable to focus the current study on the cool-down phase.

3. THERMO-MECHANICAL RESPONSE OF MMCs

The simulation of the thermo-mechanical response of MMCs during Phase 3 of the fabrication process requires nonlinear micromechanics capable of handling, among other factors, the effects of temperature, the nonlinearity of the constituent materials stress-strain behavior and the residual microstress build-up. Such an integrated micromechanics theory developed by Chamis and co-workers [10-11] is utilized in the present study. In summary, the theory proposes the following relation of in situ constituent properties P to state-variables such as temperature, stress, and time:

$$\frac{P}{P_o} = \left[\frac{T_M - T}{T_M - T_o} \right]^m \left[\frac{S - \sigma}{S_o} \right]^n \left[\frac{t_F - t}{t_F} \right]^p \quad (1)$$

The exponents in the previous equation may be estimated from experimental data. Candidate properties for this equation are the moduli, Poisson's ratios, strengths, and thermal expansion coefficients.

The micromechanics theory assumes the composite microstructure shown in Fig. 2 which consists of three material regions: the fiber, the matrix, and an interphase between them. The interphase represents either a special fiber coating or other substances such as products of chemical reactions between the fiber and matrix. Three distinct microregions may be recognized in the composite material. The three regions are shown in Fig. 2 and are identified with letters A (matrix), B (matrix-interphase), and C (matrix-interphase-

fibers). Externally applied mechanical and thermal loads on the composite will result in the development of different average stresses in the three microregions [10-11]. Because of the material non-linearity expressed by eq. 1, the calculation of composite properties and microstresses at each time step of the simulated fabrication phase requires an iterative solution of the governing equations.

4. OPTIMAL FABRICATION PROCESS

As stated previously, it is desirable to optimize the process parameters (temperature, pressure, and time) during the cool-down phase of the fabrication cycle such that: (1) the residual microstresses in the fabricated composite are favorably controlled, and (2) the integrity of the resulting composite is ensured. Considering the large number of parameters and the complexity of the simulation, this may be best accomplished with non-linear programming (NLP). A standard constrained NLP problem has the form:

$$\text{minimize } F(\mathbf{z}) \tag{2.1}$$

subjected to constraints:

$$\mathbf{z}^L \leq \mathbf{z} \leq \mathbf{z}^U \tag{2.2}$$

$$Q(\mathbf{z}) \leq \mathbf{0} \tag{2.3}$$

$$H(\mathbf{z}) = \mathbf{0} \tag{2.4}$$

where $F(\mathbf{z})$ is the objective function, $Q(\mathbf{z})$ is the inequality constraint, $H(\mathbf{z})$ is the equality constraint, and \mathbf{z} refers to a set of design variables. For our case, the design variables consist of a set of temperatures, pressures, and times sufficiently defining the cool-down phase.

The desirable state of residual microstresses is related to the projected service requirements of the composite. In the rest of the paper, the authors assume that reduction of residual microstresses is most desirable. In this context, the optimal fabrication problem is first formulated as the following constrained minimization:

$$\min(\max\{w_1\sigma_{m11}^A, w_2\sigma_{m22}^A, w_3\sigma_{m22}^B, w_4\sigma_{m22}^C\}) \tag{3}$$

subjected to fiber and matrix stress failure constraints at n_s time steps throughout the solution.

$$(S_{f11C}^C)_j < (\sigma_{f11}^C)_j < (S_{f11T}^C)_j \quad j = 1, \dots, n_s \quad (4.1)$$

$$(S_{f22C}^C)_j < (\sigma_{f22}^C)_j < (S_{f22T}^C)_j \quad j = 1, \dots, n_s \quad (4.2)$$

$$(S_{m11C}^A)_j < (\sigma_{m11}^A)_j < (S_{m11T}^A)_j \quad j = 1, \dots, n_s \quad (5.1)$$

$$(S_{m22C}^A)_j < (\sigma_{m22}^A)_j < (S_{m22T}^A)_j \quad j = 1, \dots, n_s \quad (5.2)$$

$$(S_{m22C}^B)_j < (\sigma_{m22}^B)_j < (S_{m22T}^B)_j \quad j = 1, \dots, n_s \quad (5.3)$$

$$(S_{m22C}^C)_j < (\sigma_{m22}^C)_j < (S_{m22T}^C)_j \quad j = 1, \dots, n_s \quad (5.4)$$

Upper and lower bounds on the optimization vector \mathbf{z} are also imposed in accordance with eq. 2.2.

Although eqs. 3-5 adequately represent the stated objectives, a difficulty immediately arises when a microstress increases beyond the ultimate strength value. In such a case, the material fails resulting in elimination of the load carrying capacity of the respective microregion. Therefore, the previously formulated constrained optimization problem is only meaningful within the feasible domain. Moreover, the objective function and the constraints are continuous in the feasible domain only since discontinuities occur during each failure. The discontinuity does not preclude the existence of a local minimum in the feasible domain, however, the matrix nonlinearity (eq. 1) mandates that non-linear programming algorithms designed to operate outside the feasible domain (eg. exterior penalty methods) are inapplicable to the present problem. In addition, the starting optimization process should be feasible, i.e. no microfailures should occur during fabrication. The last requirement would eliminate many of the merits of the proposed formulation in eqs. 3-5, since the prediction of an initial fabrication process without material failures may be cumbersome. In order to overcome these difficulties, the final temperature is included in the objective function (eq. 3):

$$\min(\max\{w_1 \sigma_{m11}^A, w_2 \sigma_{m22}^A, w_3 \sigma_{m22}^B, w_4 \sigma_{m22}^C\} + w_5 \frac{T_t}{T_o}) \quad (6)$$

The inclusion of final temperature in the objective function allows the use of a nonambient final temperature in the starting process. The prediction of an initial fabrication process with a sufficiently high final temperature such that microfailures do not occur is trivial. If a feasible fabrication process exists with an ambient final temperature, then the minimization of the proposed objective function will reduce the final temperature to the room value. In this manner, the associated difficulties with the knowledge of an initial feasible process are overcome and the use of the current methodology may be extended in the prediction of feasible fabrication processes.

The optimization problem described by eqs. 6 and 3-5 is numerically solved with the modified feasible directions NLP method [12]. One important feature of the modified feasible directions algorithm is that it performs a direct search within the feasible optimization domain based on the gradients of the objective function and the constraints. The algorithm includes also an active set strategy, i.e. only the constraints near violation are included in the estimation of the search direction enabling the efficient handling of the large number of constraints defined in eqs. 4-5.

5. APPLICATIONS AND DISCUSSION

This method was applied to optimize the cool-down phase of the following two unidirectional MMCs: (1) 0.40 fiber volume ratio (FVR) ultra high-modulus graphite (P100)/copper, and (2) 0.40 FVR SiC/Ti15-3-3-3. Fabrication data regarding the current fabrication processes of these composites were provided by the Materials Division of NASA Lewis Research Center. Representative constituent properties of both composite systems at reference conditions (70°F, 0 psi) are shown in Tables 1 and 2.

For the analysis, phase 3 was subdivided into four increments of linearly varying temperature and pressure. Stress constraints were imposed at five evenly spaced time intervals in each linear segment. In this manner, twenty constraints were introduced for each microstress inequality described in eqs. 4-5. Only the residual microstresses σ_{m11}^A and σ_{m22}^A were included in the objective function (eq. 6), that is: $w_1 = w_2 = w_5 = 1$ and $w_3 = w_4 = 0$. The temperatures, pressures, and times at the starting and final points of

the four linear segments were used as optimization parameters. The temperature at the beginning of Phase 3 was held constant and equal to the respective temperature of the current processes, and the final pressure was set equal to zero. The following upper and lower bounds were imposed on the optimization variables in accordance with eq. 2.2:

$$T_o \leq T \leq T_M \quad (7.1)$$

$$0 \leq p \leq 50ksi \quad (7.2)$$

$$10sec \leq t \leq 18000sec \quad (7.3)$$

Case 1: P100/Copper

Fig. 3 shows the current and the resultant optimum fabrication process for the P100/copper MMC. The cool-down phase of the current process consists of two segments of linearly decreasing temperature and pressure. In the resultant optimum process the temperature remains high during the first 2000sec, is reduced to room temperature in the following 2500sec, and remains there until the end of the process. The predicted optimal consolidation pressure in Fig. 3b is significantly higher than the pressure of the current process. At 0sec the pressure is 1.58ksi, in the next 4500sec the pressure gradually increases to 6.5ksi, and then drops to zero. The pressure increases as the temperature decreases makes sense, because in this manner the matrix becomes highly nonlinear and undergoes "plastic" deformation resulting in reduced matrix microstress σ_{m11}^A . The predicted build-ups of microstresses σ_{m11}^A and σ_{m22}^A are shown in Fig. 4. The final microstresses in Fig. 4 are the residual microstresses in the fabricated composite. The residual microstress σ_{m11}^A of the optimal process decreased by 14.5% compared to the respective microstress value of the current process. The residual microstress σ_{m22}^A of the optimal process was increased and both residual microstresses of the optimum process have nearly equal values. The predicted microstress build-up in the current process is more uniform compared to the optimum process because both pressure and temperature decrease almost linearly, as opposed to the more complicated temperature-pressure variation of the optimal process. Figs. 5 and 6 illustrate the variation of the longitudinal and transverse in situ matrix moduli and

strengths respectively during the current and the optimal process. The fact that the matrix in the optimal process is undergoing nonlinear deformations is further illustrated in Fig. 5 by the variation of the in situ moduli. The high residual microstresses resulted in a significant decrease of the matrix longitudinal modulus in both current and optimal processes. The optimal process has a higher final in situ matrix longitudinal modulus, and decreased final transverse modulus compared to the current process. The in situ strengths of the matrix did not change.

Case 2: SiC/Ti15-3-3-3

The resultant optimum process for SiC/Ti15-3-3-3 is shown in Fig. 7 together with the current one. The microstress build-up is shown in Fig. 8, and the variations of the in situ moduli and strengths are respectively shown in Figs. 9 and 10. In contrast to the previous case, the process optimization did not result in any significant reductions of the final microstresses with respect to the currently used process. A possible explanation is that the current process may have been improved through a trial-and-error procedure.

As previously stated, the principal physical mechanism that has contributed to microstress reductions in the previous case studies was the non-linear in situ matrix behavior, as a result of high temperature and pressure. Two additional physical phenomena not included in the present study, namely the matrix solidification history and viscoplasticity, affect the microstress development in the composite. During the first stages of the cool-down phase when the temperature and pressure are high, the matrix actually remains in a near fluid state, and temperature and pressure variations do not contribute to the development of residual microstresses. In fact, the resultant optimal process for the graphite/copper composite indicates that the matrix moduli should remain low during the first stages of the process and illustrates the need for incorporating the matrix solidification history during the fabrication. Prolonged matrix nonlinearity will also result in partial relaxation of the induced thermal matrix microstresses. The effects of matrix solidification history require further consideration. Work is currently under development to include this effect in the simulation and optimization of the fabrication process.

6. SUMMARY

A method is proposed for optimizing the fabrication process of unidirectional metal-matrix composites. The response of the fabricated MMC was simulated based on nonlinear micromechanics. The temperature and pressure variation during the cool-down phase of the fabrication process was optimized for reduced residual microstresses in the fabricated composite and elimination of failures. An in-house research code has been developed incorporating this method.

Case studies were performed on ultra-high modulus graphite (P100)/copper, and silicon carbide (SiC)/titanium (Ti15-3-3-3) composites. The predicted optimal process for graphite/copper resulted in an estimated reduction of the maximum final microstress by 15%, by favorably optimizing the nonlinear in situ matrix behavior. The optimization of the fabrication process for SiC/Ti15-3-3-3 produced insignificant reductions in the residual microstresses.

REFERENCES

1. I. M. Daniel, Y. Liber and C. C. Chamis, "Measurement of Residual Strains on Boron/Epoxy and Glass/Epoxy Laminates," *Composite Reliability Conference, ASTM*, 1974.
2. H. T. Hahn and N. J. Pagano, "Curing Stresses in Composite Laminates," *Journal of Composite Materials*, Vol. 9, pp. 91-106, 1975.
3. A. C. Loos and G. S. Springer, "Curing of Epoxy Matrix Composite," *Journal of Composite Materials*, Vol. 17, pp. 135-169, 1983.
4. J. A. Nairn and P. Zoller, "Matrix Solidification and the Resulting Thermal Stresses in Composites," *Journal of Material Science*, Vol. 20, pp. 355-367, 1985.
5. T. J. Chapman, et. al., "Thermal Skin/Core Residual Stresses Induced During Cooling of Thermoplastic Matrix Composites," *Proceedings of the American Society for Composites, Third Technical Conference*, pp. 449-458, 1988.

6. K. S. Kim, H. T. Hahn and R. B. Groman, "The Effect of Cooling Rate on Residual Stresses in a Thermoplastic Composite," *Journal of Composite Technology and Research*, Vol. 11, No. 2, pp. 47-52, 1989.
7. W. D. Brewer and J. Unnam, "Metallurgical and Tensile Property Analysis of Several Silicon Carbide/Titanium Composite Systems," *Proceedings of 111th AIME Annual Meeting, Mechanical Behavior of Metal-Matrix Composites*, Warrendale, PA, Feb. 1982, pp.39-50.
8. C. C. Chamis, P. L. N. Murthy and D. A. Hopkins, "Computational Simulation of High Temperature Metal Matrix Composites Cyclic Behavior", *NASA TM 1022115*, 1988.
9. Y. Weitsman and D. Ford, "On the Optimization of Cool-Down Temperatures on Viscoelastic Resins," *Proceedings of 14th Annual Meeting of the Society of Engineering Science, Inc.*, pp.323-336, 1977.
10. D. A. Hopkins and C. C. Chamis, "A Unique Set of Micromechanics Equations for High Temperature Metal Matrix Composites", *NASA TM 87154*, 1985.
11. P. L. N. Murthy, D. A. Hopkins and C. C. Chamis, "Metal Matrix Composite Micromechanics: In-Situ Behavior Influence on Composite Properties," *NASA TM 102302*, 1989.
12. G. N. Vanderplaats, *Numerical Optimization Techniques for Engineering Design: With Applications*, McGraw-Hill Book Company, New York, 1984.

Table 1. Representative constituent mechanical properties of P100 Graphite/Copper at reference conditions.

P100 Graphite	Copper
$E_{f11} = 105.0 \text{ Mpsi}$	$E_m = 17.7 \text{ Mpsi}$
$E_{f22} = 0.90 \text{ Mpsi}$	
$G_{f12} = 1.10 \text{ Mpsi}$	$G_m = 6.81 \text{ Mpsi}$
$G_{f23} = 0.70 \text{ Mpsi}$	
$\rho_f = 0.078 \text{ lb/in}^3$	$\rho_m = 0.32 \text{ lb/in}^3$
$\nu_{f12} = 0.20 \text{ in/in}$	$\nu_m = 0.30 \text{ in/in}$
$\nu_{f23} = 0.25 \text{ in/in}$	
$\alpha_{f11} = -0.90 \text{ } \mu\text{in/in}/^\circ\text{F}$	$\alpha_m = 9.80 \text{ } \mu\text{in/in}/^\circ\text{F}$
$\alpha_{f22} = 5.60 \text{ } \mu\text{in/in}/^\circ\text{F}$	
$S_{f11,T} = 325.0 \text{ ksi}$	$S_{mn} = 32.0 \text{ ksi}$
$S_{f11,C} = 200.0 \text{ ksi}$	
$S_{f22} = 25.0 \text{ ksi}$	
$S_{f12} = 25.0 \text{ ksi}$	$S_{ms} = 19.0 \text{ ksi}$
$S_{f23} = 12.5 \text{ ksi}$	

Table 2. Representative constituent mechanical properties of SiC/Ti15-3-3-3 at reference conditions.

SiC	Ti15-3-3-3
$E_{f11} = 62.0 \text{ Mpsi}$	$E_m = 12.3 \text{ Mpsi}$
$E_{f22} = 62.0 \text{ Mpsi}$	
$G_{f12} = 23.8 \text{ Mpsi}$	$G_m = 4.659 \text{ Mpsi}$
$G_{f23} = 23.8 \text{ Mpsi}$	
$\rho_f = 0.11 \text{ lb/in}^3$	$\rho_m = 0.172 \text{ lb/in}^3$
$\nu_{f12} = 0.30 \text{ in/in}$	$\nu_m = 0.32 \text{ in/in}$
$\nu_{f23} = 0.30 \text{ in/in}$	
$\alpha_{f11} = 1.80 \text{ } \mu\text{in/in}/^\circ\text{F}$	$\alpha_m = 4.50 \text{ } \mu\text{in/in}/^\circ\text{F}$
$\alpha_{f22} = 1.80 \text{ } \mu\text{in/in}/^\circ\text{F}$	
$S_{f11,T} = 500.0 \text{ ksi}$	$S_{mn} = 130.0 \text{ ksi}$
$S_{f11,C} = 650.0 \text{ ksi}$	
$S_{f22,T} = 500.0 \text{ ksi}$	
$S_{f22,C} = 650.0 \text{ ksi}$	
$S_{f12} = 300.0 \text{ ksi}$	$S_{ms} = 90.0 \text{ ksi}$
$S_{f23} = 300.0 \text{ ksi}$	

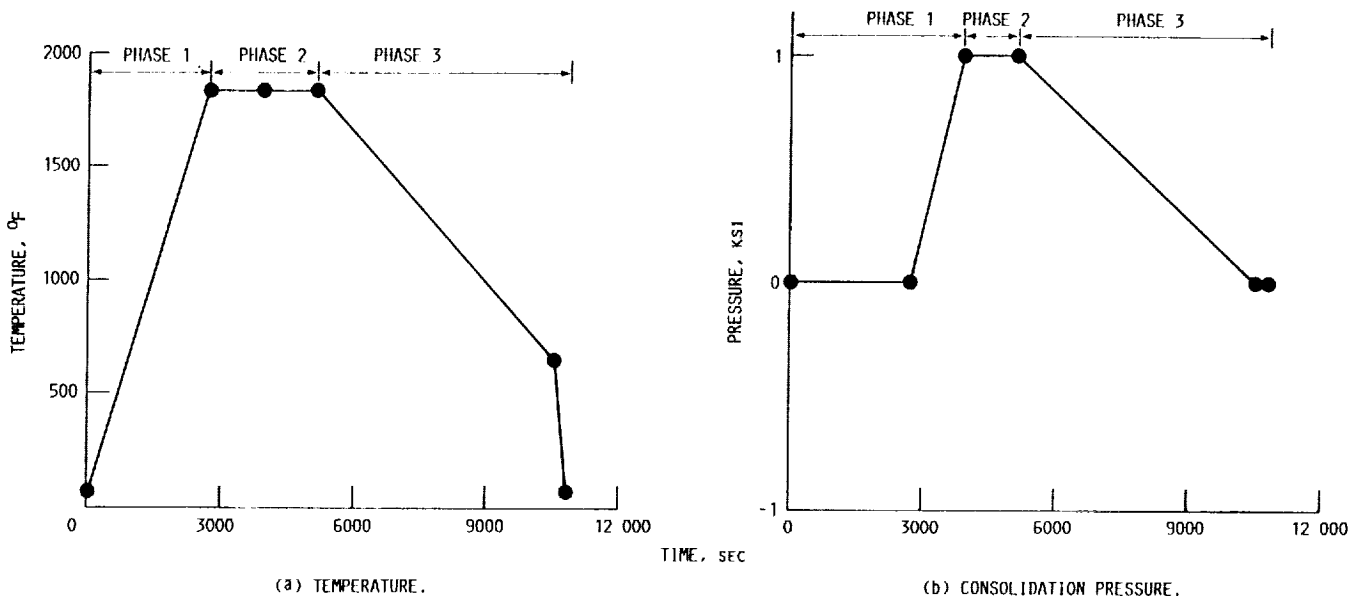


FIGURE 1. - TYPICAL PROCESSING CYCLE FOR GRAPHITE/COPPER COMPOSITE.

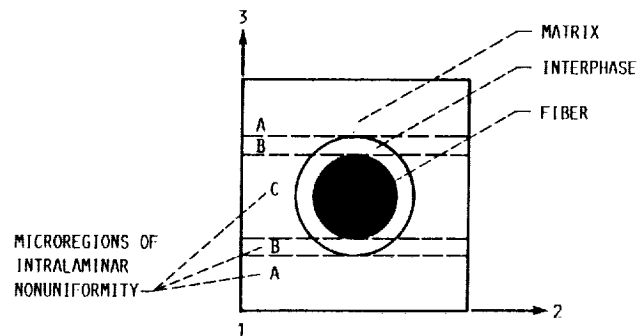
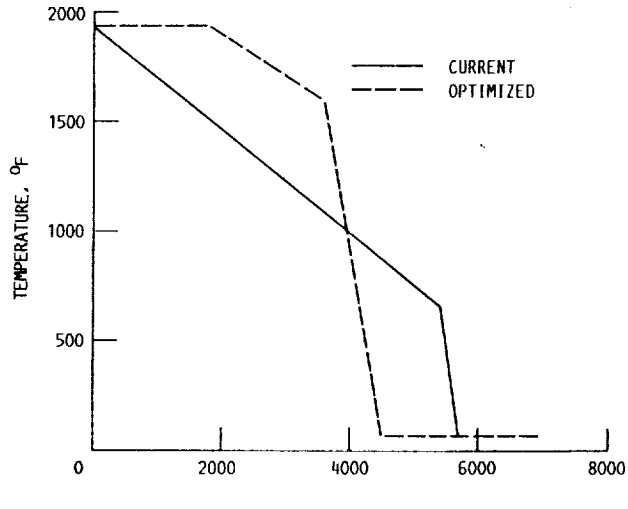
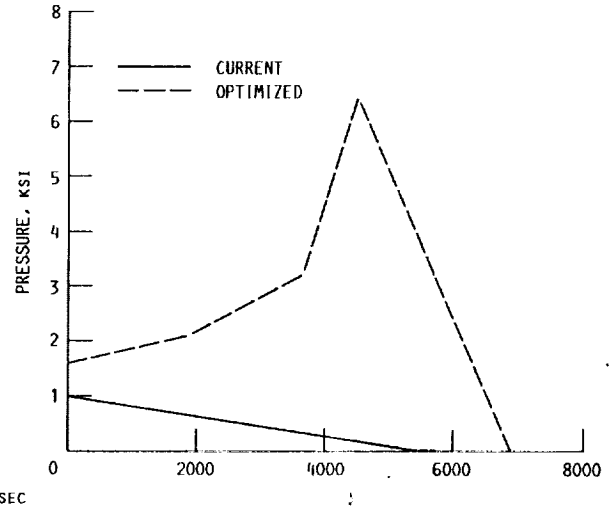


FIGURE 2. - MATERIAL MICROREGIONS IN A REPRESENTATIVE METAL-MATRIX COMPOSITE CELL.



(a) TEMPERATURE.



(b) CONSOLIDATION PRESSURE.

FIGURE 3. - OPTIMUM AND CURRENT COOL-DOWN PHASES FOR 0.40 FVR P100/COPPER (CASE 1).

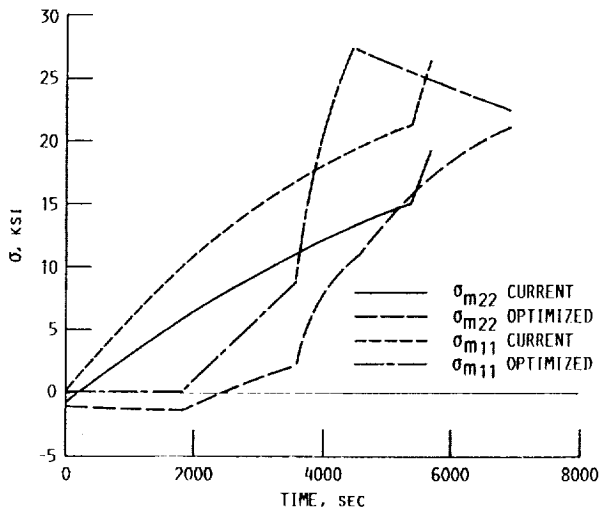


FIGURE 4. - MATRIX MICROSTRESSES DEVELOPED DURING THE COOL-DOWN PHASE OF 0.40 FVR P100/COPPER (CASE 1). OPTIMUM AND CURRENT PROCESSES.

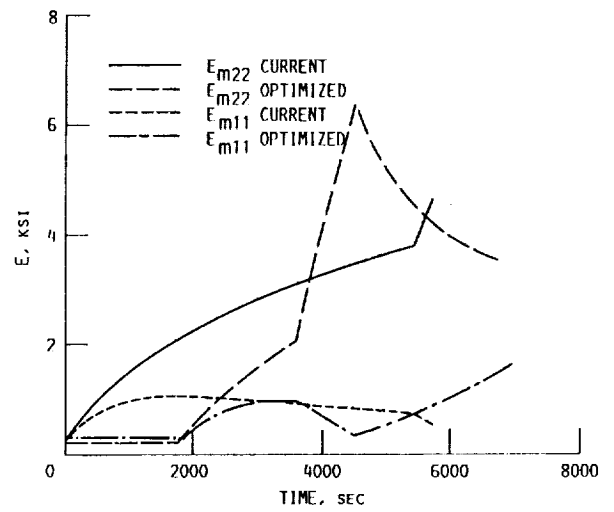


FIGURE 5. - IN SITU MATRIX MODULI DURING THE COOL-DOWN PHASE OF 0.40 FVR P100/COPPER (CASE 1). OPTIMUM AND CURRENT PROCESSES.

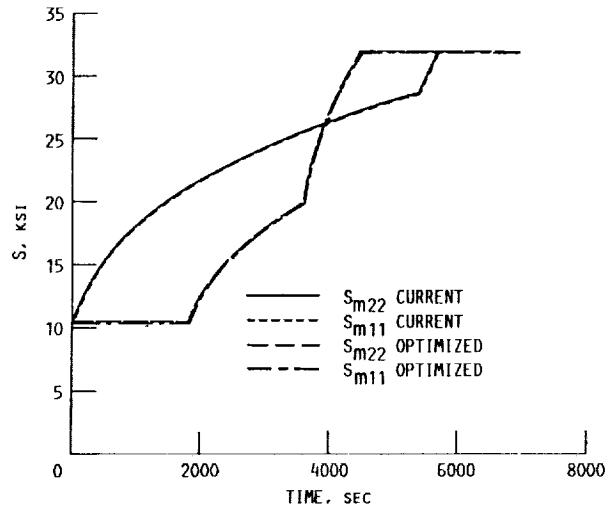
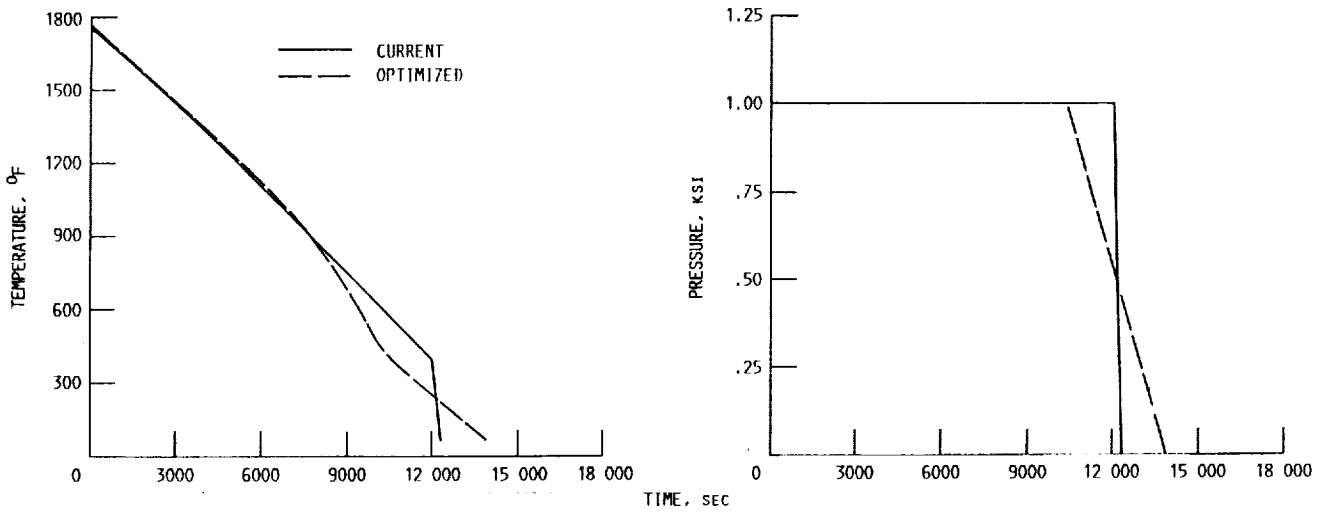


FIGURE 6. - IN SITU MATRIX STRENGTHS DURING THE COOL-DOWN PHASE OF 0.40 FVR P100/COPPER (CASE 1). OPTIMUM AND CURRENT PROCESSES.



(a) TEMPERATURE.

(b) CONSOLIDATION PRESSURE.

FIGURE 7. - OPTIMUM AND CURRENT COOL-DOWN PHASES FOR 0.40 FVR SiC/Ti15-3-3 (CASE 2).

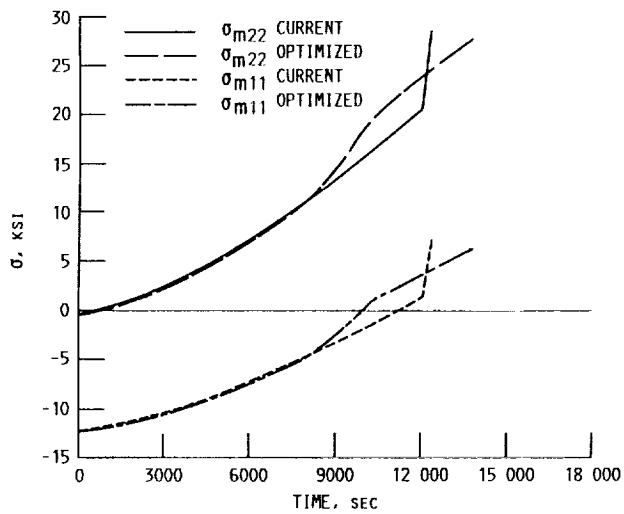


FIGURE 8. - MATRIX MICROSTRESSES DEVELOPED DURING THE COOL-DOWN PHASE OF 0.40 FVR SiC/Ti15-3-3-3 (CASE 2). OPTIMUM AND CURRENT PROCESSES.

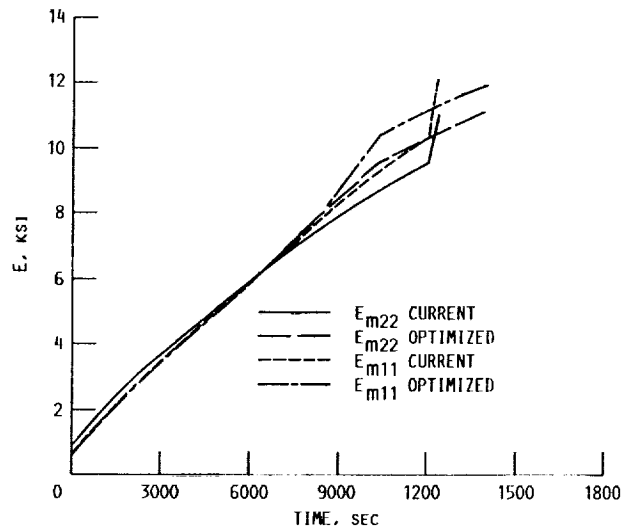


FIGURE 9. - IN SITU MATRIX MODULI DURING THE COOL-DOWN PHASE OF 0.40 FVR SiC/Ti15-3-3-3 (CASE 2). OPTIMUM AND CURRENT PROCESSES.

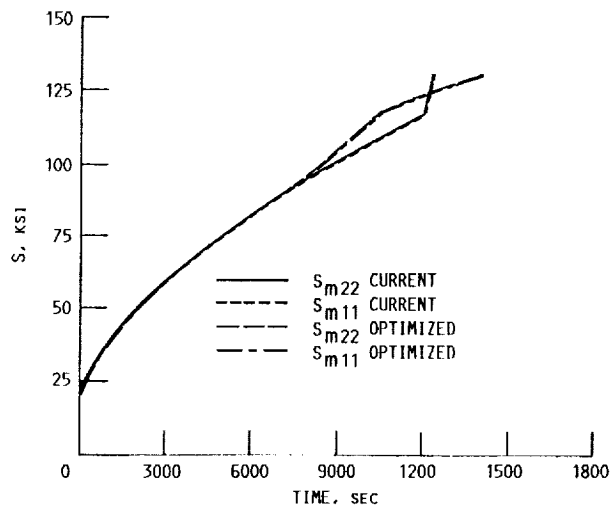


FIGURE 10. - IN SITU MATRIX STRENGTHS DURING THE COOL-DOWN PHASE OF 0.40 FVR SiC/Ti15-3-3-3 (CASE 2). OPTIMUM AND CURRENT PROCESSES.



Report Documentation Page

1. Report No. NASA TM-102559		2. Government Accession No.		3. Recipient's Catalog No.	
4. Title and Subtitle Optimal Fabrication Processes for Unidirectional Metal-Matrix Composites: A Computational Simulation				5. Report Date	
				6. Performing Organization Code	
7. Author(s) D.A. Saravanos, P.L.N. Murthy, and M. Morel				8. Performing Organization Report No. E-5379	
				10. Work Unit No. 510-01-0A	
9. Performing Organization Name and Address National Aeronautics and Space Administration Lewis Research Center Cleveland, Ohio 44135-3191				11. Contract or Grant No.	
				13. Type of Report and Period Covered Technical Memorandum	
12. Sponsoring Agency Name and Address National Aeronautics and Space Administration Washington, D.C. 20546-0001				14. Sponsoring Agency Code	
15. Supplementary Notes Prepared for the 35th International SAMPE Symposium and Exhibition, Anaheim, California, April 2-5, 1990, D.A. Saravanos, Case Western Reserve University, Cleveland, Ohio 44106 and NASA Resident Research Associate at Lewis Research Center. P.L.N. Murthy, NASA Lewis Research Center. M. Morel, Sverdrup Technology, Inc., NASA Lewis Research Center Group, Cleveland, Ohio 44135.					
16. Abstract A method is proposed for optimizing the fabrication process of unidirectional metal-matrix composites. The temperature and pressure histories are optimized such that the residual microstresses of the composite at the end of the fabrication process are minimized and the material integrity throughout the process is ensured. The response of the composite during the fabrication is simulated based on a nonlinear micromechanics theory. The optimal fabrication problem is formulated and solved with non-linear programming. Application cases regarding the optimization of the fabrication cool-down phases of unidirectional ultra-high modulus graphite/copper and silicon carbide/titanium composites are presented.					
17. Key Words (Suggested by Author(s)) Metal-matrix composites; Fabrication; Optimization; Optimal temperature; Optimal consolidation pressure; Residual stresses; Nonlinear micromechanics			18. Distribution Statement Unclassified - Unlimited Subject Category 24		
19. Security Classif. (of this report) Unclassified		20. Security Classif. (of this page) Unclassified		21. No. of pages 18	22. Price* A03